CHALMERS
UNIVERSITY OF TECHNOLOGY

Steering behavior-based fatigue detection

Evaluation and implementation for drowsy driver warning system

Master's thesis in Mobility engineering

Sanjana Hassan Ananda Kumar

DEPARTMENT OF MECHANICS AND MARITIME SCIENCES

CHALMERS UNIVERSITY OF TECHNOLOGY
Gothenburg, Sweden 2025
www.chalmers.se

Master's Thesis in Mobility engineering

Steering behavior-based fatigue detection

Evaluation and implementation for drowsy driver warning system

Sanjana Hassan Ananda Kumar

CHALMERS
UNIVERSITY OF TECHNOLOGY

Department of Mechanics and Maritime Sciences
Chalmers University of Technology
Gothenburg, Sweden 2025

Steering behavior-based fatigue detection
Evaluation and implementation for drowsy driver warning system
Sanjana Hassan Ananda Kumar

Supervisor: Mats Jonasson, Mechanics & Maritime Sciences
David Öst, Volvo Group Trucks Technology

Examiner: Mats Jonasson, Mechanics & Maritime Sciences

Master's Thesis 2025
Department of Mechanics and Maritime Sciences
Chalmers University of Technology
SE-412 96 Gothenburg
Sweden
Telephone +46 31 772 1000

Cover: A driver information display prompting the driver to take a break after the driver alert support system detects signs of fatigue.

Typeset in LaTeX
Gothenburg, Sweden 2025

Steering behavior-based fatigue detection
Evaluation and implementation for drowsy driver warning system

Sanjana Hassan Ananda Kumar
Department of Mechanics and Maritime Sciences
Chalmers University of Technology

Abstract

This research was conducted to analyze steering behavior as an alternative approach to detecting driver drowsiness. The thesis examined standard metrics such as steering wheel angle, steering wheel angle rate, yaw rate, and lane position—variables directly and indirectly related to steering behavior—to assess how much information they bear about drowsiness. A derived metric, the steering reversal rate, was also analyzed to further explain the effects of drowsiness. These metrics demonstrated a strong correlation with driver drowsiness, which was subjectively measured using the Karolinska Sleepiness Scale (KSS).

Based on this analysis, two parameters derived from the steering reversal rate—micro and macro corrections—were used to develop two methods for detecting drowsiness. These parameters were significant because, as a driver becomes drowsier, the frequency of micro-corrections tends to decrease, while macro-corrections increase.

Two methods have been developed to detect a drowsy driver based on the above analysis. The first method employed a logistic regression model, using the absolute values of micro and macro corrections to directly correlate with the KSS ratings. This approach did not account for temporal patterns and treated the data independently of its time-series nature. In contrast, the second method incorporated a time-series perspective by evaluating changes in micro and macro correction rates over time rather than relying on their absolute values. During development, it was observed that vehicle speed significantly influenced steering behavior. At lower speeds, even non-drowsy drivers exhibited more macro corrections and fewer micro-corrections. However, at speeds above 65 km/h, non-drowsy drivers typically made more micro-corrections and fewer macro-corrections. This insight enhanced the robustness of the second method, wherein vehicle speed was considered one of the contributing factors in analyzing driver steering behavior. Additionally, the second method involved a learning phase for each individual driver, allowing for personalized threshold values. This driver-specific calibration improved adaptability.

Overall, the second method of real-time analysis of changes in micro and macro correction rates proved to be a more effective and reliable approach, yielding better results than the current system(based on lane distance) for detecting driver drowsiness.

Keywords: steering reversal rate, micro-corrections, macro-corrections, logistic regression model, real-time analysis, personalized thresholds.

Preface

This thesis represents the culmination of my deepening interest in human-centered vehicle design, an area that first captured my attention during my internship at Volvo. What began as a curiosity quickly grew into a focused academic and practical endeavor, shaped by real-world challenges and meaningful collaboration.
Throughout this project, I have had the opportunity to explore the complex relationship between driver behavior and vehicle systems, an experience that has been both intellectually rewarding and personally enriching. The process has tested my problem-solving abilities, expanded my technical knowledge, and reinforced the importance of user-centered approaches in engineering design.
I am sincerely grateful to everyone who supported me throughout this journey—both professionally and personally. Their guidance, encouragement, and patience made this work possible.

Acknowledgements

I would like to sincerely thank my academic supervisor and examiner, Mats Jonasson, whose professional insight and enthusiasm were instrumental throughout the duration of my thesis.
I am truly grateful to David Öst, the industrial supervisor at the Volvo Group, for offering me this remarkable opportunity and challenge. The supportive environment he created was key to the successful completion of my work.
Finally, I extend my heartfelt thanks to my dear friends and family for their unwavering support and encouragement. Their presence gave me the strength to navigate uncertainties and persevere through challenges, even in the most difficult moments.

Sanjana Hassan Ananda Kumar, Gothenburg, June 2025

List of Acronyms

Below is the list of acronyms that have been used throughout this thesis, listed in alphabetical order:

AUC	Area Under Curve
FFT	Fast Fourier Transform
KSS	Karolinska Sleepiness Scale
ODE	Ordinary Differential Equation
PDF	Probability Density Function
ROC	Receiver Operating Characteristic
SRR	Steering Reversal Rate

Nomenclature

Below is the nomenclature of indices, sets, parameters, and variables that have been used throughout this thesis.

Indices

n,i	Indices for each data point

Parameters

τ	Time constant
α	Filter coefficient
σ	Standard deviation
ϵ	A small positive constant
μ	Mean
β_n	n_{th} coefficient or weight of the model

Signals

θ_i	Steering wheel angle at occurrence i

Contents

List of Figures

List of Tables

1
Introduction

This thesis investigates the detection of driver fatigue through the analysis of vehicle steering behavior. It explores various methods for identifying signs of drowsiness based on the driver's interaction with the vehicle.
The study begins with the collection of data from multiple test logs from several vehicles, followed by signal processing of relevant signals such as steering wheel angle, yaw rate, and lane position. Secondary parameters derived from these signals are then analyzed for their potential to indicate driver fatigue. A thorough examination of the correlation between these parameters and driver drowsiness is performed to provide a basis for the proposed detection methods.
Building upon this understanding, several methods were developed to address the problem of detecting driver fatigue. The first approach involves the development of a logistic regression model, which uses secondary steering parameters—specifically the micro and macro steering reversal rates—as predictors for driver drowsiness. The second approach involves monitoring changes in the driver's steering behavior over time, using these same parameters to identify potential signs of fatigue. The third method estimates the expected steering wheel angle of an alert driver and detects deviations from this expected behavior as indicators of drowsiness.
To assess the performance of the proposed methods, a comparative analysis is undertaken, emphasizing their respective strengths and limitations with regard to sensitivity—reflecting the accuracy in identifying truly drowsy drivers—and specificity—indicating the effectiveness of correctly recognizing non-drowsy drivers. This analysis provides insight into the effectiveness of each approach and highlights areas for potential improvement.

1.1 Background

Driver fatigue is recognized as one of the major causes of road accidents worldwide. According to the U.S. National Highway Traffic Safety Administration, approximately 100,000 accidents each year are attributed to drowsy driving, resulting in more than 1,500 fatalities and over 70,000 injuries [1]. These statistics underscore the urgent need to develop effective methods for detecting and alerting fatigued drivers, especially in the context of long-distance, night-time, or monotonous driving conditions where the risk is particularly high.
Driver fatigue can be broadly categorized into three types: active task-related, passive task-related, and sleep-related. Active task-related fatigue results from high task demands, such as navigating through heavy traffic, poor visibility, or engag-

ing in secondary tasks while driving. Passive task-related fatigue occurs in low-stimulation environments, such as long stretches of highway, monotonous driving conditions, or prolonged periods of underload [7]. Sleep-related fatigue stems from biological factors, including circadian rhythms, sleep deprivation, sleep restriction, and sleep disorders [2].

The detection of driver fatigue poses significant challenges, as the onset can be gradual and vary greatly between individuals. Fatigue may not always be consciously recognized by the driver, making it difficult to rely solely on self-reported assessments. In response to this, fatigue detection techniques are commonly categorized into three main types: subjective, physiological, and performance-based measures.

Subjective measures involve self-assessment tools such as the 7-point Stanford Sleepiness Scale and the 9-point Karolinska Sleepiness Scale [8]. While these methods are easy to administer, they depend on the driver's awareness and honesty, limiting their reliability in real-time scenarios. Physiological measures, such as monitoring brain activity (EEG), heart rate variability, and eye movements (e.g., blink duration, pupil diameter), offer high accuracy but typically require intrusive sensors or specialized equipment, which may not be practical for everyday use.

Performance-based measures, in contrast, analyze the driver's interaction with the vehicle. These include variations in steering wheel movement, vehicle speed, lane deviation, and brake response. Such measures are non-intrusive and can be obtained directly from in-vehicle sensors, making them well-suited for real-time monitoring in real-world applications.

In particular, steering behavior has shown promise as a potential indicator of driver fatigue [5, 6]. Subtle changes in steering reversal rates, smoothness, and lane-keeping behavior may reflect a decline in alertness. As modern vehicles are increasingly equipped with advanced sensors and control systems, leveraging these built-in capabilities for fatigue detection presents a cost-effective and scalable solution.

Therefore, it is both practical and worthwhile to investigate vehicle-based signals—such as steering wheel angle—to assess their effectiveness in identifying signs of driver fatigue. Unlike physiological or subjective measures, these signals are readily accessible and require no additional hardware or input from the driver, making them a compelling area of focus for fatigue detection systems.

1.2 Purpose

The purpose of this thesis is to enhance the existing methods [9] of detecting driver fatigue currently implemented at Volvo Group Trucks Technology by incorporating additional vehicle-based parameters. Specifically, it investigates the use of steering wheel angle, along with other relevant signals, to improve the accuracy and reliability of drowsy driving detection. By leveraging these parameters, the thesis aims to develop a more effective and robust approach for real-time identification of driver drowsiness.

1.3 Goals

To guide the research and provide a clear direction for the work presented, this thesis is structured around the following primary goals:

- To evaluate and quantify the effectiveness of using steering wheel angle as an alternative parameter for estimating driver fatigue.
- To implement and test a driver alert system based on steering wheel angle for the real-time detection of drowsy driving.

1.4 Research objectives

To gain a deeper understanding of the relationship between steering behavior and driver fatigue, it is essential to address several key research questions that will guide the investigation:

- Is there a noticeable change in the steering pattern when the driver is drowsy compared to when the driver is alert? This question aims to explore the fundamental relationship between steering behavior and driver alertness, which is crucial for understanding how steering wheel angle can be used to estimate fatigue.
- How is the changing steering pattern correlated with the driver's level of drowsiness? This question focuses on quantifying the correlation between steering patterns and varying degrees of fatigue, supporting the goal of implementing an effective driver alert system.
- Is the correlation between steering pattern and driver drowsiness level consistent across all drivers, or does it vary depending on individual characteristics? Addressing this question will help determine whether a generalized model can be applied to all drivers or if individualized approaches are necessary for accurate fatigue detection.

By answering these questions, this thesis aims to achieve its goals of evaluating the use of steering wheel angle as a reliable parameter for detecting driver fatigue and implementing a real-time driver alert system.

1.5 Limitations

While this thesis presents promising approaches for detecting driver drowsiness based on steering behavior, several limitations must be acknowledged that may affect the generalization and practical applicability of the findings:

- The scope of this thesis is limited to the analysis of available drowsy and non-drowsy test data. As real-world driving conditions are not considered, the conclusions drawn may not fully capture the complexity of practical scenarios.
- The assessment of driver drowsiness in this study is based solely on the Karolinska Sleepiness Scale. Consequently, the observed correlations between steering behavior and drowsiness may not be generalizable to other drowsiness measurement methods.

- The steering behavior analysis used in this research does not differentiate between drowsiness and driver distraction. As a result, instances of distraction may be misinterpreted as signs of fatigue.
- This thesis focuses exclusively on the development of a drowsiness detection system that issues visual or auditory alerts to the driver, without implementing any physical intervention. Therefore, the system's effectiveness may be limited in cases where the driver ignores the warnings and continues to drive while fatigued.

2

Data preparation and analysis

The following sections outline the steps involved in preparing and analyzing the data. This encompasses processing raw signals, extracting secondary features, and evaluating their relationship with driver drowsiness.

2.1 Data collection

The log data used in this analysis were collected from driver alert support tests conducted on heavy duty commercial vehicles in 2022 at a 5-kilometer-long ovular test track designed to replicate motorway driving conditions, as per the test methods outlined in Commission Delegated Regulation (EU) 2021/134 [3]. The dataset comprises 44 test drives conducted by 27 drivers, with no more than two test runs per individual. The test data were collected under conditions where few drivers became progressively drowsier over time, while some recovered slightly during the drive.
The key signals extracted from the test data include steering wheel angle, yaw rate, and lane position, all of which were down-sampled to a frequency of 10 Hz. In addition to these vehicle signals, the Karolinska Sleepiness Scale (KSS) ratings, provided by the drivers throughout the driver alert support tests, were also recorded. Unlike the vehicle signals, which were obtained directly from sensors, the KSS ratings were communicated verbally by the drivers every 10 minutes. This approach served as an alternative to the interval prescribed by EU regulations. A 10-minute interval was chosen to minimize driver distraction compared to the recommended 5-minute interval, while still maintaining adequate measurement accuracy.

Rating	Verbal Description
1	Extremely alert
2	Very alert
3	Alert
4	Rather Alert
5	Neither alert nor sleepy
6	Some signs of sleepiness
7	Sleepy, no effort to keep awake
8	Sleepy, some effort to keep awake
9	Very sleepy, great effort to keep awake, fighting sleep

Figure 2.1: Karolinska Sleepiness Scale

2.2 Data processing

Two types of data were processed in this study: (1) raw signals, and (2) the KSS ratings provided verbally by the driver.

Signal processing of raw signals

Signal processing of the raw signals involved frequency analysis using Fast Fourier Transform, spectrogram, and filtering the signals using the Euler backward method.

- Fast Fourier Transform (FFT) was applied to the raw signals of steering wheel angle, yaw rate, and lane position to analyze their frequency components. The FFT results revealed that the steering wheel angle signal exhibited higher-magnitude components primarily at very low frequencies (below 0.5 Hz). A similar low-frequency dominance was also observed in the yaw rate and lane position signals at even lower frequencies. This implies that yaw rate and lane position are slower dynamics compared to that of steering wheel angle.

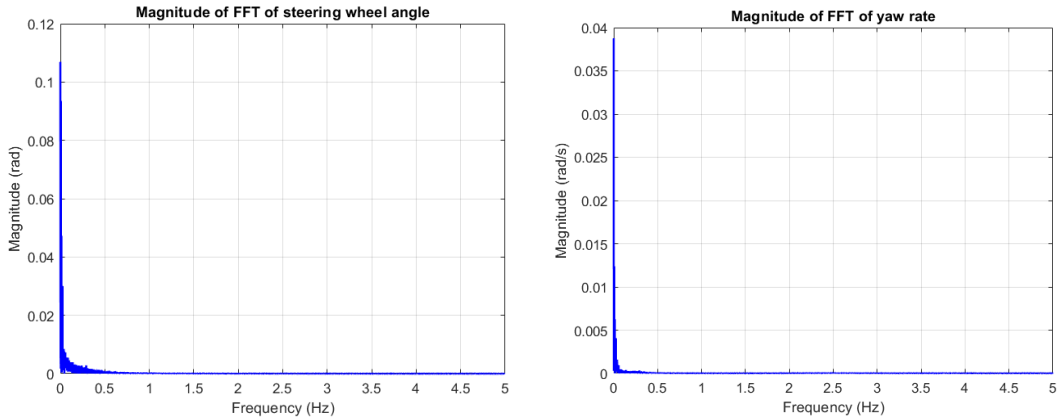

Figure 2.2: Fast Fourier Transform of steering wheel angle and yaw rate of one test sample

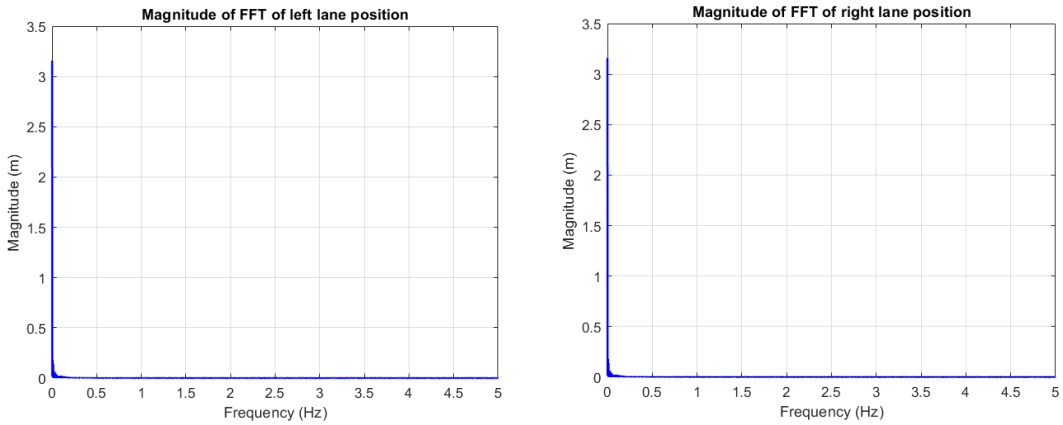

Figure 2.3: Fast Fourier Transform of left and right lane positions of one test sample

- A spectrogram was applied to the raw signals of steering wheel angle, yaw rate, and lane position to analyze how their frequency content changes over time. The results indicated that, over time, higher-frequency components with increased amplitude in the steering wheel angle became more prominent, suggesting a rise in rapid and pronounced steering corrections. In contrast, the yaw rate and lane position signals continued to exhibit low-frequency content, but the magnitude of these frequencies increased over time, suggesting growing intensity in the vehicle's motion and lane deviation.

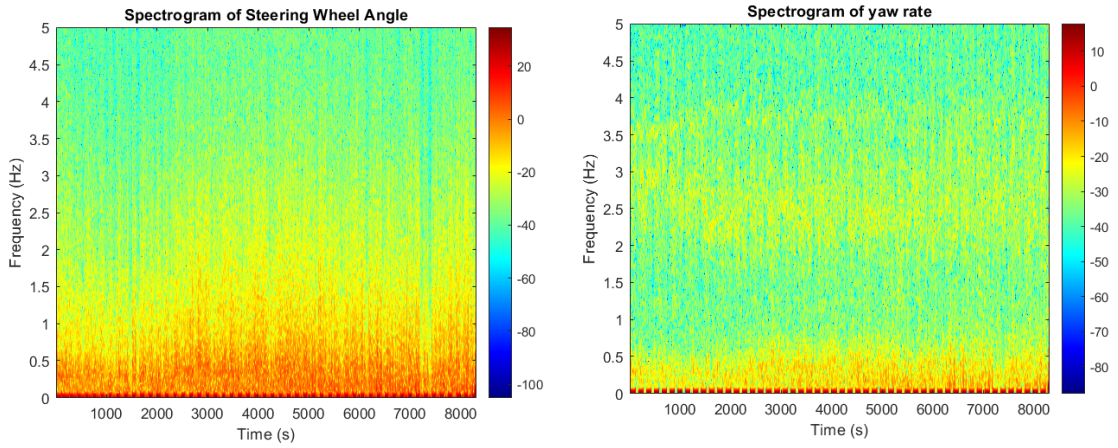

Figure 2.4: Spectrogram of steering wheel angle and yaw rate of one test sample

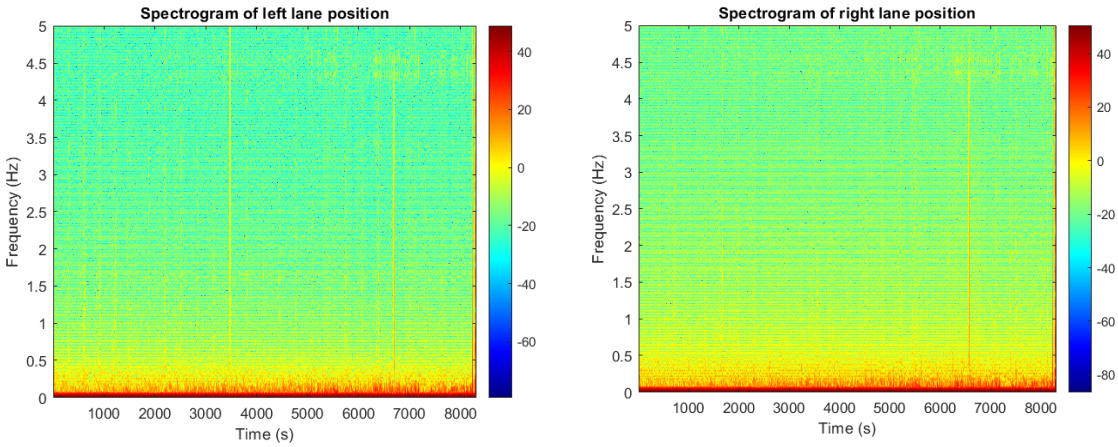

Figure 2.5: Spectrogram of left and right lane positions of one test sample

The FFT analysis indicated that yaw rate and lane position primarily consist of lower-frequency components compared to the steering wheel angle signal. The spectrogram analysis further revealed that, over time, the frequency content of the steering wheel angle signal increases, while the magnitudes of the yaw rate and lane position signals also become stronger. These observations support the initial hypothesis that steering behavior and related vehicle dynamics change as the driver becomes drowsier, thereby addressing the first research objective.

Although the FFT and spectrogram are presented for a single test sample, the results are representative and can be generalized to the majority of test samples.

- Signal filtering using Euler backward method - To further investigate the underlying behavior, it was essential to filter the signals using the Euler backward method. This approach helps eliminate the influence of road curvature and environmental factors, allowing the analysis to focus primarily on the vehicle's intrinsic dynamics.

  The Euler backward method, also known as the implicit Euler method, is a first-order numerical technique used to solve ordinary differential equations (ODEs) of the form:

  $$\frac{dx}{dt} = f(x, t)$$

  The method estimates the value of the variable at the next time step using the derivative at the next time step:

  $$x_{n+1} = x_n + h \cdot f(x_n + 1, t_n + 1)$$

  where:
  - x_n is the current value of the variable,
  - h is the step size or time increment,
  - $f(x_n + 1, t_n + 1)$ is the derivative or rate of change at the next point.

  The Euler backward method is explicit, meaning it does not require solving an equation to get the next value. This makes it computationally efficient but less stable for stiff systems or high-frequency data.

  In signal processing, however, the Euler backward method can be adapted to function as a first-order low-pass filter by discretizing a simple differential equation:

  $$\tau \frac{dy}{dt} + y = x$$

  where:
  - x is the input signal,
  - y is the output (filtered) signal,
  - τ is the time constant controlling the smoothness of the filter.

  Applying the Euler backward discretization yields the following recursive formula:

  $$y[n] = \alpha \cdot x[n] + (1 - \alpha) \cdot (y[n - 1])$$

  where:
  - $x[n]$ is the input signal at time step n,

- $y[n]$ is the filtered output signal at time step n,
- $y[n-1]$ is the filtered output signal at time step $n-1$,
- $\alpha = \frac{h}{\tau+h}$ is the filter coefficient,
- h is the sampling time interval.
- τ is the time constant, which controls the cutoff frequency and responsiveness of the filter.

The filter coefficient α determines how quickly the filter responds to changes in the input. A smaller α results in stronger smoothing, while a larger α allows more of the original signal's variation to pass through.

The Euler backward method can also be adapted to implement a first-order high-pass filter. Starting from the continuous-time high-pass filter differential equation:

$$\tau\frac{dy}{dt} + y = \tau\frac{dx}{dt}$$

Discretizing this using the Euler backward method gives the recursive formula:

$$y[n] = \alpha \cdot (y[n-1] + x[n] - x[n-1])$$

where:

- $x[n]$ is the input signal at time step n,
- $x[n-1]$ is the input signal at time step n,
- $y[n]$ is the filtered output signal at time step n,
- $y[n-1]$ is the filtered output signal at time step n
- $\alpha = \frac{\tau}{\tau+h}$ is the high-pass filter coefficient,
- h is the sampling time interval,
- τ is the time constant, which controls the cutoff frequency and responsiveness of the filter.

In this form, the filter allows rapid changes in the input signal (i.e., high-frequency components) to pass while attenuating slow or steady-state components. A smaller α results in stronger attenuation of low frequencies, while a larger α passes more of the input signal's high-frequency content.

Based on this method, a recursive low-pass filter with a cutoff frequency of 5 Hz was developed to derive normalized key signals, while a recursive high-pass filter with a cutoff frequency of 0.1 Hz was used to derive secondary steering metrics. These cutoff frequencies were selected based on the correlation between the normalized key signals, secondary steering metrics, and the driver's KSS ratings.

(The normalization of key signals and the derivation of secondary steering metrics are explained in detail in section 2.3)

```
%low-pass filter

 prev_filtered_value = signal(1);

 for i=1:length(signal)

         fs = 10;        % sampling frequency
         cutoff = 5;     % cut-off frequency
         alpha = 1 / (1 + fs / (2 * pi * cutoff));  % filter coefficient alpha
         filtered_signal = alpha * signal(i) + (1 - alpha) * prev_filtered_value;  % low pass filtered value
         prev_filtered_value = filtered_signal;

 end
```

Figure 2.6: Recursive low pass filter - MATLAB code

```
%high-pass filter

 prev_filtered_value = signal(1);

 for i=2:length(signal)

         fs = 10;        % sampling frequency
         cutoff = 0.1;     % cut-off frequency
         alpha = fs / (fs + (2 * pi * cutoff));  % filter coefficient alpha
         filtered_signal = (alpha) * (signal(i)- signal(i-1) +  prev_filtered_value);  % high pass filtered value
         prev_filtered_value = filtered_signal;

 end
```

Figure 2.7: Recursive high pass filter - MATLAB code

The above images are the MATLAB codes used for recursive high-pass and low-pass filters. The sampling and cut-off frequencies are measured in Hz.

Karolinska Sleepiness Scale rating interpolation

The Karolinska Sleepiness Scale (KSS) was verbally reported by the drivers at 10-minute intervals. To create a continuous representation of the KSS scores, the data were interpolated between these 10-minute intervals, under the assumption that changes in KSS scores occur in a continuous manner rather than discretely. Interpolation was carried out using the MATLAB command `interp`. Two different scales were used for the interpolation: one with a least count of one minute, and the other with a finer resolution of 0.1 seconds. This approach allowed for a more granular analysis of the variations in sleepiness levels over time.

2.3 Data transformation

The processed data was transformed into a more suitable and structured form, ensuring that the ground truth remained intact. This transformation involved the normalization of signals into relevant key indices, thereby mitigating the effects of external factors such as road curvature and environmental conditions.

Concurrently, a secondary steering metric, referred to as the steering reversal rate, was derived using the methodology proposed by Gustav Markkula [4] This metric demonstrated a correlation with drowsiness comparable to that of lane position,

further strengthening the analytical framework.

The following section provides a comprehensive explanation of these methodologies and their application in the context of the study.

- Key indices were computed recursively for steering wheel angle, steering wheel angle rate, yaw rate and lane positions. Key index is defined as below -

$$\text{key\_index} = \frac{\sigma}{\max\left(\text{LPF}_{\text{signal}},\ \varepsilon\right)}$$

where,
σ represents the real time standard deviation of the input signal (steering wheel angle, steering wheel angle rate, yaw rate or lane positions signals).
$\text{LPF}_{\text{signal}}$ denotes the low-pass filtered signal using Euler backward method.
ε is a small positive constant introduced to avoid division by zero.

The standard deviation represents excess variation in the signal and the division by the signal itself is done to compensate for various road curvatures that require a certain value.

The key index was computed at a sampling rate of 0.1 seconds for the steering wheel angle, steering wheel angle rate, and yaw rate, while the lane positions were sampled every minute. This discrepancy in sampling rates is due to the differing dynamics of the parameters. The steering wheel angle, steering wheel angle rate, and yaw rate exhibit faster changes and, therefore, require a higher sampling frequency to capture their variations accurately. In contrast, lane position changes at a much slower rate, and its trends become perceptible only when averaged over a longer period, such as one minute. Consequently, a minute-based sampling interval for lane position is sufficient to capture its dynamics without unnecessary data redundancy.

The cutoff frequency for the low pass filter was selected to be as high as 5 Hz, which corresponds to the maximum Nyquist frequency for the given sampling rate. Additionally, the value of epsilon was chosen to be as small as possible, approaching zero. (It is important to note that all epsilon values were selected based on a trial-and-error approach, supplemented by informed judgment tailored to the specific metric being evaluated). This resulted in the key indices being elevated, as dividing by a value close to zero yields a large quotient. Despite this, the observed trends in the key indices closely aligned with the ground truth data, ensuring that the calculated values accurately reflected the underlying system behavior.

- Steering reversal rate (SRR) is generally defined as the number, per minute, of change in steering wheel direction larger than a certain minimum angular value, referred to as the gap size [4].

The gap size was chosen to range between 1° and 10°. Any angle exceeding this range was considered indicative of steering actions rather than a reversal. Specifically, the SRR for gap sizes smaller than 3° was referred to as the SRR of micro-corrections, while the SRR for gap sizes greater than 6° was referred to as the SRR of macro-corrections.

The first step in calculating the SRR involved filtering the signals using a recursive high-pass filter, based on the Euler backward method (as described in the previous section). This approach effectively removed low-frequency steering wheel angle changes, which are typically associated with the driver's actions during turns. Determining the appropriate cutoff frequency for the high-pass filter posed a challenge. To address this, a reverse methodology was employed: the cutoff frequency was selected by identifying the frequency that maximized the correlation between the SRR and KSS ratings. Through this process, it was determined that a cutoff frequency of 0.1 Hz yielded the highest correlation. Refer figure.

Once the signals were filtered, the method prescribed by Gustav Markkula [4] was employed to calculate the Steering Reversal Rate (SRR). According to this method, the first step involves identifying the stationary points within the signal. This process was carried out as described below:

$$\frac{\theta_i - \theta_{i-1}}{\Delta t} \geq 0, \qquad \frac{\theta_i - \theta_{i+1}}{\Delta t} \geq 0$$

to determine the local maxima

$$\frac{\theta_i - \theta_{i-1}}{\Delta t} \leq 0, \qquad \frac{\theta_i - \theta_{i+1}}{\Delta t} \leq 0$$

to determine the local minima

where ,

θ_i: The value of steering wheel angle at the current time step i.
θ_{i-1}: The value of steering wheel angle at the previous time step $i-1$.
θ_{i+1}: The value of steering wheel angle at the previous time step $i+1$.
Δt: The time difference between two consecutive time steps, representing the interval over which the change in steering wheel angle is measured.

Here Δt was ignored, assuming a constant time interval, as each data point was sampled at regular intervals. Consequently, the above equations were reduced to:

$$\theta_i - \theta_{i-1} \geq 0, \qquad \theta_i - \theta_{i+1} \geq 0$$

and

$$\theta_i - \theta_{i-1} \leq 0, \qquad \theta_i - \theta_{i+1} \leq 0$$

This simplification was made to focus on the differences between successive data points without explicitly considering the time interval between them.

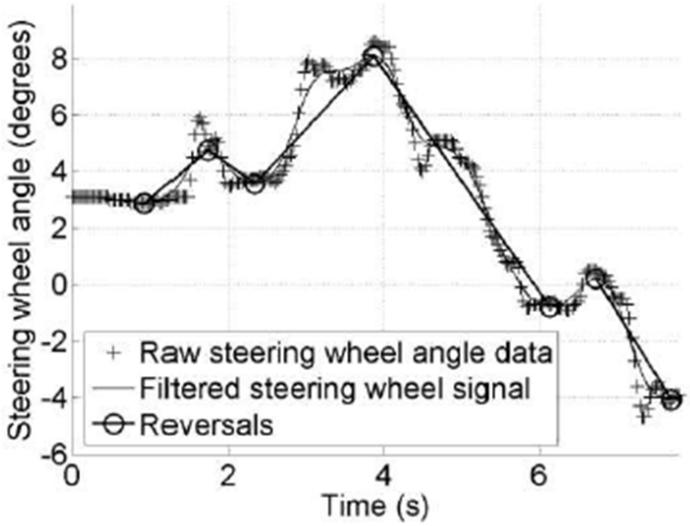

Figure 2.8: Steering reversal rate measurement according to Gustav Markkula and Johan Engström method cite here

Once the stationary points were identified, the corresponding distances between local minima and maxima, which exceeded the specified gap size, were measured to calculate the upward reversals. Similarly, the distances between local maxima and minima greater than the gap size were measured to compute the downward reversals. The upward and downward reversals were then summed to determine the total number of reversals per minute.

This was calculated for all gap sizes ranging from 1° to 10° in order to identify the angle that yielded the maximum correlation.

Data transformation into key indices and secondary steering metrics was essential to eliminate the external influences because by eliminating these influences, the data became more consistent, thus enhancing the robustness of the correlation analysis.

2.4 Data correlation

Establishing the correlations between the key indices, steering reversal rate, and driver drowsiness—represented by the Karolinska Sleepiness Scale (KSS) rating—was essential for developing a system to detect driver drowsiness. Furthermore, this formed the second research objective: to investigate how the steering wheel angle and its related variables vary with the driver's level of drowsiness.

This section provides a detailed explanation of the methodology employed to conduct this analysis.

The correlation between the key indices of steering wheel angle, yaw rate, lane position and the KSS rating was assessed solely through visual analysis using box-and-whisker plots. One of the reasons for this approach was because statistical correlations among these variables could not be established, as the average values of steering wheel angle, steering wheel angle rate, and yaw rate remained nearly constant throughout the testing procedure. This constancy was due to the uniform shape of the test track. As a result, any statistical correlation derived from these variables would have been inconsequential and was therefore not pursued.

With regard to lane position, visualizing the changing trend was deemed sufficient, as lane position is a derived parameter influenced by steering behavior. Moreover, the focus of this thesis was primarily on utilizing steering-related parameters for the development of a drowsiness detection system, rather than relying directly on lane position.

In contrast, for the steering reversal rate, the linear statistical correlation coefficient— Pearson correlation coefficient—was calculated in addition to the box plot visualization. This was justified by the observation of a consistent increase in the average values of these metrics with increasing levels of driver drowsiness.

In addition, the key indices were computed recursively at 0.1-second intervals, with the KSS ratings interpolated accordingly. Simultaneously, the steering reversal rate and the key index of lane position were calculated on a per-minute basis, and the KSS ratings were interpolated in line with these calculations.

Correlation of key indices of steering wheel angle, steering wheel angle rate, yaw rate, and lane position with driver drowsiness

- Steering wheel angle - The key index of the steering wheel angle was defined using an epsilon value of 1^{-26}, which is effectively zero. Consequently, the results can be regarded as closely explaining the actual vehicle behavior. For each test drive, the average of the maximum key index corresponding to each KSS rating was computed. Subsequently, the distribution of these values was determined across all drivers.
  As illustrated in figure 2.9 , there was a consistent increase in the maximum

key index of the steering wheel angle, with a notable rise observed from KSS level 6 to KSS level 7.

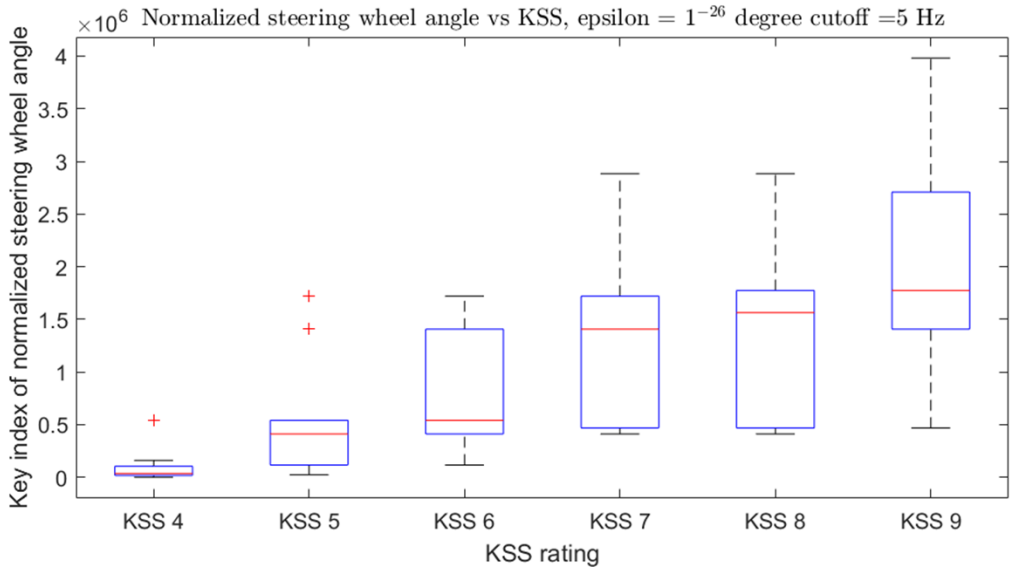

Figure 2.9: Maximum key index of normalized steering wheel angle vs KSS rating

- Steering wheel angle rate - This was computed as the rate of change of steering wheel angle as below -

$$\frac{\theta_i - \theta_{i-1}}{\Delta t} = \theta'_i$$

where,

θ_i: The value of steering wheel angle at the current time step i.
θ_{i-1}: The value of steering wheel angle at the previous time step $i-1$.
Δt: The time difference between two consecutive time steps, representing the interval over which the change in steering wheel angle is measured. It is equal to 0.1 seconds.
θ'_i: The rate of change of steering wheel angle at time step i.

As evident in figure 2.10 , there was a gradual increase in the maximum key index of normalized steering wheel angle rate with KSS rating.

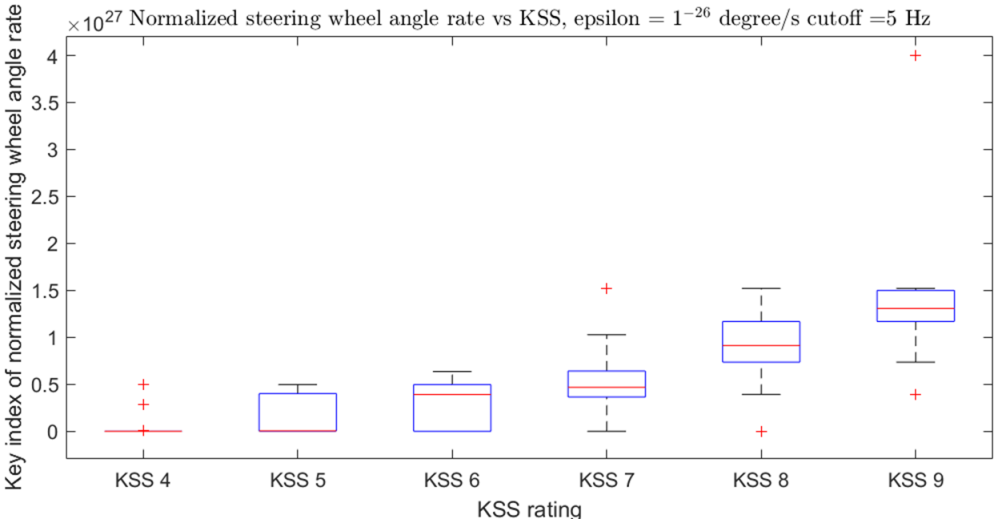

Figure 2.10: Maximum key index of normalized steering wheel angle rate vs KSS rating

- Yaw rate - The key index of the yaw rate was defined using an epsilon value of 1^{-6}, which is close to zero. Consequently, the results can be regarded as closely explaining the actual vehicle behavior. For each test drive, the average of the maximum key index corresponding to each KSS rating was computed. Subsequently, the distribution of these values was determined across all drivers.

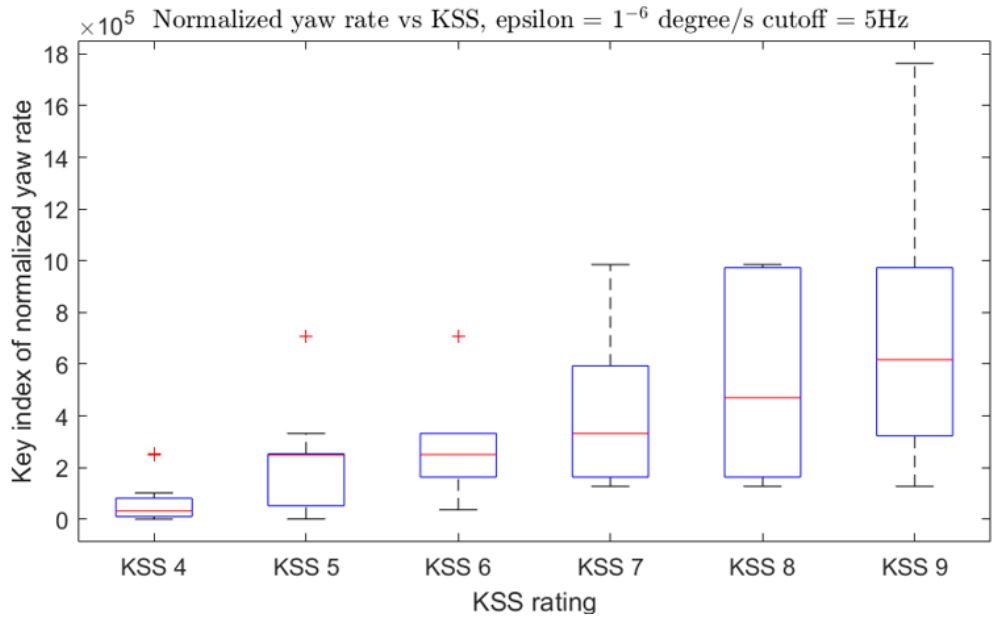

Figure 2.11: Maximum key index of normalized yaw rate vs KSS rating

As seen in figure 2.11, there was a gradual increase in the maximum key index of normalized yaw rate with KSS rating.

- Lane position - The key index of lane position—considering both the left and right boundaries—was defined using an epsilon value of 0.1 meters, which is relatively small in the context of vehicular distance measurements. As a result, the computed values can be considered to closely explain the actual vehicle behavior. For each test drive, the average of the maximum key index associated with each KSS rating was calculated. Thereafter, the distribution of these values was analyzed across all drivers.
  The key indices were computed at two temporal resolutions: 0.1-second intervals and 1-minute intervals. It was observed that the trend became more pronounced at the 1-minute interval, supporting the notion that lane position reflects an accumulated behavioral pattern over time. Refer to figures 2.12 and 2.13 .

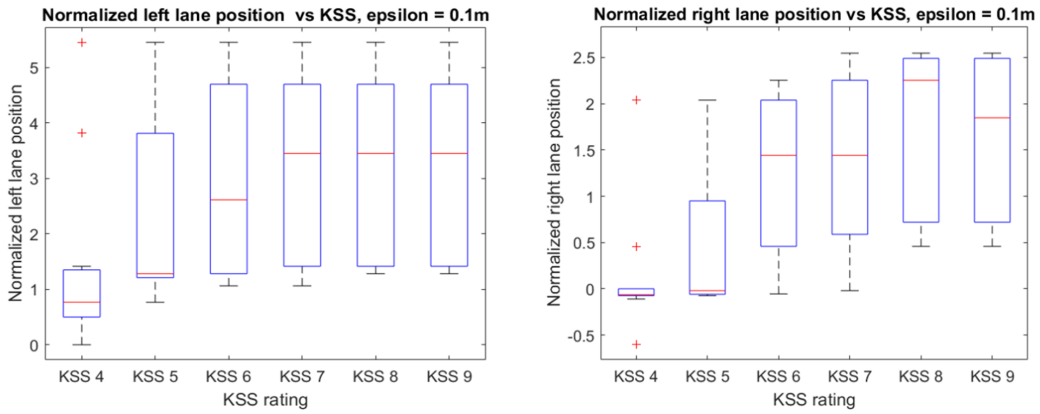

Figure 2.12: Key index of lane positions computed at 0.1 second interval

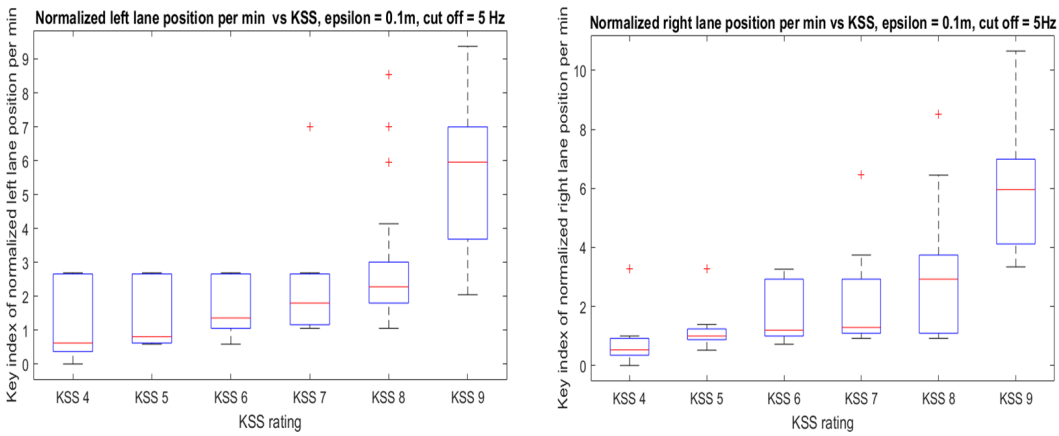

Figure 2.13: Key index of lane positions computed at 1 minute interval

As shown in figure 2.13 , a significant increase in the key index of lane position was observed beginning at KSS level 8. This suggests that lane deviation is an accumulated behavior that becomes more pronounced as the level of driver drowsiness increases.

The analysis of the key indices of steering-related parameters indicates that, as driver drowsiness increases, greater variations in both steering wheel angle and lane position are observed. Additionally, a monotonic increase in steering wheel angle rate and yaw rate is evident. It is important to note that this trend represents an average across all drivers. While the overall pattern is consistent among drivers, the specific values of the key indices may vary between individuals.

Correlation between steering reversal rate and driver drowsiness

The steering reversal rate was calculated as described in Section 2.3 (Data Processing). To evaluate its correlation with driver drowsiness, two complementary approaches were employed. First, a statistical method was used by computing the Pearson correlation coefficient to quantify the linear correlation across various gap sizes. Second, a visual analysis was conducted by plotting the distribution of steering reversal rates at the gap size exhibiting the highest correlation, in order to gain a clearer understanding of the overall trend.

- Statistical correlation - To quantify the correlation between the steering reversal rate at various gap sizes and KSS ratings, a linear relationship was assumed between the two variables. This assumption is supported by existing research \cite{ref}. The correlation was quantified using the Pearson correlation coefficient, a statistical measure of linear correlation, which is defined as follows:

$$r = \frac{\sum_{i=1}^{n}(x_i - \bar{x})(y_i - \bar{y})}{\sqrt{\sum_{i=1}^{n}(x_i - \bar{x})^2}\sqrt{\sum_{i=1}^{n}(y_i - \bar{y})^2}}$$

  where,

  - r is the Pearson correlation coefficient.
  - x_i and y_i are the individual sample points from the variables X - steering reversal rate at various gap sizes and Y- KSS ratings given by the driver, respectively.
  - $\bar{x}$ and $\bar{y}$ are the means (averages) of the variables X and Y.
  - n is the number of data points.
  - $\sum$ denotes summation, indicating that we sum over all n data points.

  Both steering reversal rate and KSS ratings were filtered using a moving average filter with a window size of 35. This window size was selected based on the correlation strength, ensuring a balance between the number of data points included in the average and preventing the inclusion of the entire dataset at once.

  Figure 2.14 shows how the size of the moving average window affects the Pearson correlation coefficient.

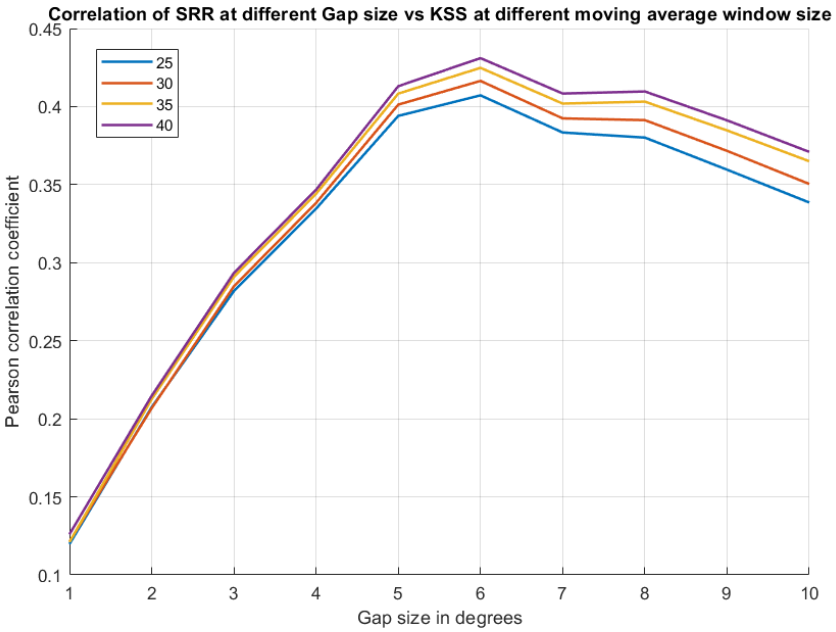

Figure 2.14: Correlation of SRR with KSS rating at different sizes of moving average window

Analysis of the correlation data across all drivers reveals that each driver exhibits a maximum correlation at a different gap size. However, the highest average correlation observed across all drivers is 0.4248, corresponding to a gap size of 6°. (Data attached in appendix A)
Figure 2.16 shows how the cut-off frequency of the high pass filter affects the Pearson correlation coefficient.

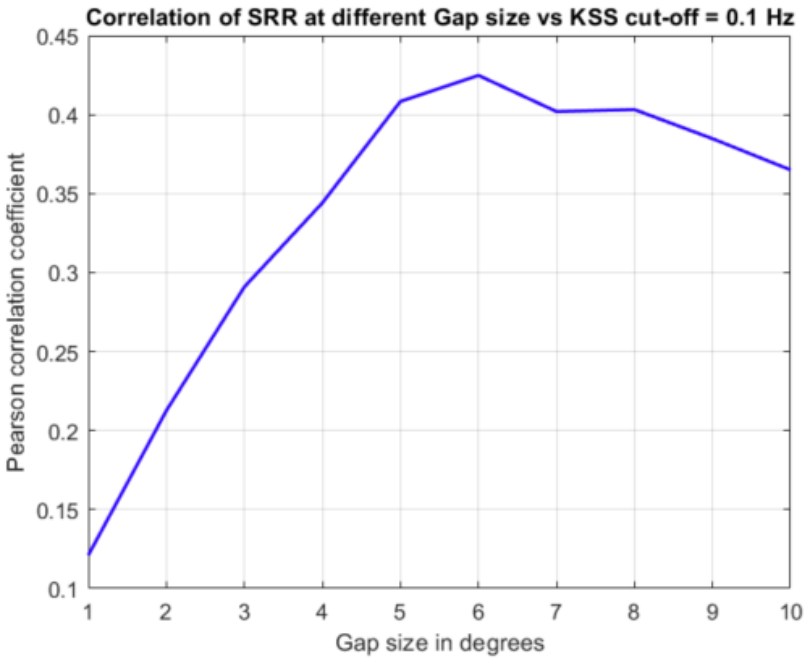

Figure 2.15: Highest average correlation coefficient vs Gap size

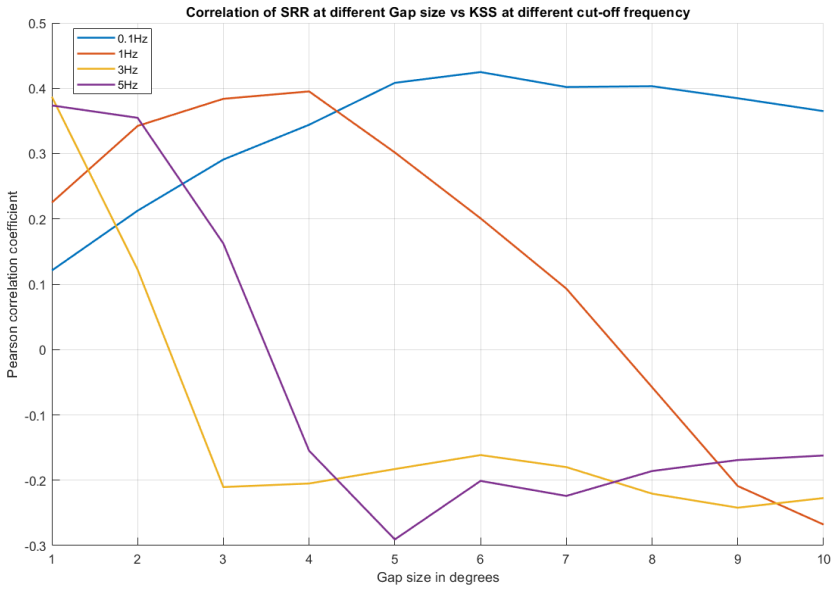

Figure 2.16: Correlation coefficients vs gap size at different cut off frequencies for steering wheel angle filtering

- Visual analysis of the steering reversal rate was conducted using box plots to have a better understanding of the overall trend of steering reversal rate with KSS rating. For this analysis, the average steering reversal rate corresponding to each KSS rating was computed individually for each driver. Subsequently, the distribution of these averaged values was examined across all drivers. The analysis was performed for two categories of gap sizes: those greater than 6°, referred to as macro corrections, and those less than 3°, referred to as micro corrections.

  As shown in figure 2.17, the average steering reversal rate at gap size greater than 6°—referred to as macro-corrections—was observed to increase with higher KSS ratings. This suggests that drivers tend to make a greater number of large-amplitude steering corrections as their level of drowsiness increases. Additionally, it is noteworthy that the distribution of macro-corrections became narrower with increasing KSS levels. This indicates that, at higher levels of drowsiness, most drivers exhibited similar ranges of macro-corrective steering behavior.

  In contrast to macro-corrections, the average steering reversal rate at gap sizes less than 3°—referred to as micro-corrections—was generally observed to decrease with increasing KSS ratings. However, as illustrated in figure 2.18, there is a noticeable increase in micro-corrections prior to a decline beginning at KSS level 6. This anomaly is attributed to lower driving speeds (below 65 km/h) during the initial phases of the test, as well as missing data points in some test logs corresponding to KSS levels 4 and 5.

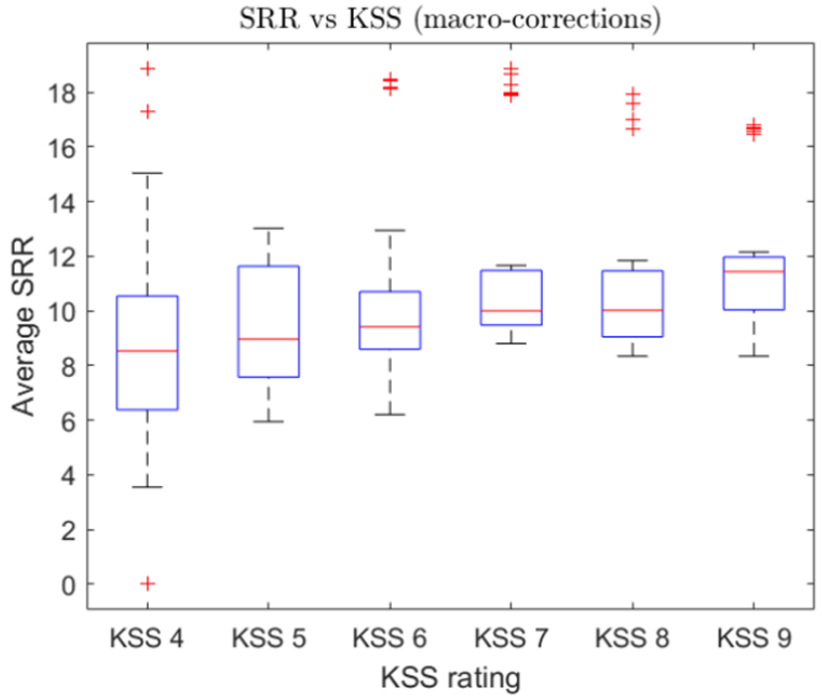

Figure 2.17: Steering reversal rate vs KSS ratings distribution of macro corrections

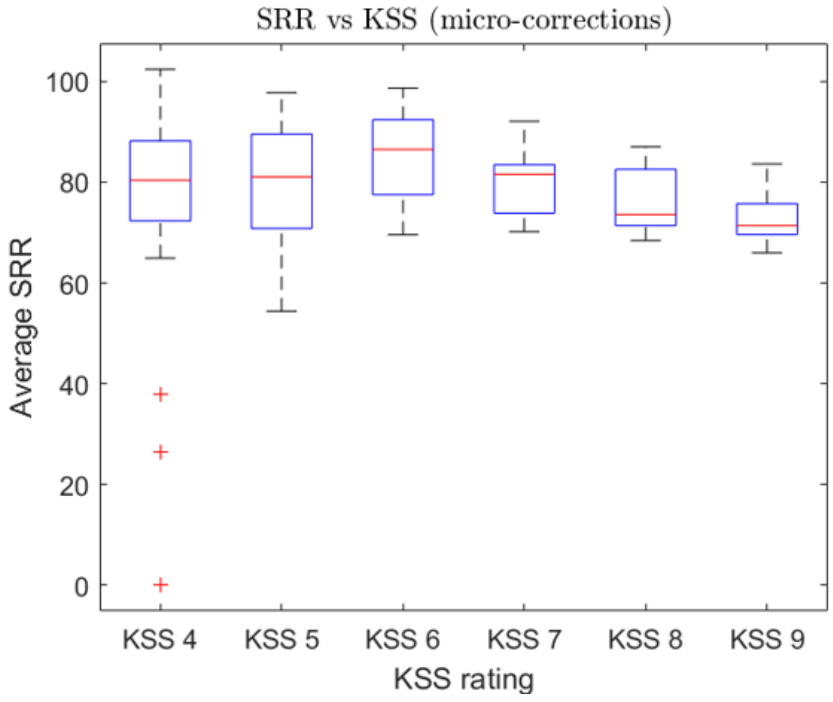

Figure 2.18: Steering reversal rate vs KSS ratings distribution of micro corrections

The analysis of the correlation between various steering-related parameters and driver drowsiness revealed a clear and measurable change in these parameters with increasing levels of drowsiness. Specifically, most parameters—including the key

indices of steering wheel angle, steering wheel angle rate, yaw rate, lane position, and the steering reversal rate associated with macro-corrections—increased as driver drowsiness intensified. In contrast, the steering reversal rate associated with micro-corrections showed a decreasing trend.

Although these patterns could be generalized across drivers, the distribution plots showed that the extent of change in each parameter varied depending on individual driving characteristics. This variability highlighted the influence of personal driving styles on the manifestation of drowsiness-related behaviors. The findings from this analysis addressed the third research question outlined at the beginning of the study.

3

Algorithm design and implementation

Based on the analysis presented in the preceding section, various algorithms were explored to detect driver drowsiness, employing three distinct approaches. The first approach utilized a machine learning technique, specifically logistic regression. The second approach involved analyzing driver behavior through the application of a probability density function. The third approach entailed the development of a driver model using pure pursuit control. This section provides a detailed explanation of each of the implemented algorithms.

3.1 Logistic regression model

The test data was analyzed using two different approaches: as time series data and as continuous data by aggregating all test data into a single, unified dataset, thereby disregarding the temporal dimension. For the purpose of implementing a logistic regression model, the latter approach was adopted, treating the data as one comprehensive dataset without accounting for time-based variations.

The dataset comprised of two predictor variables—steering reversal rates associated with micro-corrections and macro-corrections—and one output variable, the Karolinska Sleepiness Scale (KSS) rating.

The process of building the logistic regression model involved the following key steps:

3.1.1 Data cleaning

This was a critical step due to inconsistencies in the sampling frequencies of different features. Specifically, the Karolinska Sleepiness Scale (KSS) ratings were not recorded as frequently as the steering wheel angle measurements. To address this discrepancy, the lengths of the two variables were aligned to ensure consistency across the dataset. Additionally, all data corresponding to KSS ratings below 5 was excluded to eliminate potentially unreliable or inconsistent observations, thereby enhancing the overall quality and reliability of the dataset.

3.1.2 Data preparation

– In this step, the data was transformed, relevant features were selected, and feature scaling was applied. The two predictor variables—steering reversal rates of micro- and macro-corrections—required scaling, as their values differed by an order of magnitude of ten or more. To address this, standardization was performed using the Z-score method. This technique transforms the data using the following formula:

$$z = \frac{x - \mu}{\sigma}$$

where,
z is the standardized value (Z-score)
x is the original data point
μ is the mean of the feature
σ is the standard deviation of the feature

The predictor variables initially included both the raw predictor variables and additional features derived from them. Feature selection was subsequently performed using correlation matrices to identify the most relevant variables for model development. Based on the results of this analysis, three logistic regression models were constructed, each using a different combination of features, as outlined below:

Model 1 -
x_1: Normalized steering reversal rate of macro corrections,
x_2: Normalized steering reversal rate of micro corrections

Model 2 -
x_1: Normalized steering reversal rate of macro corrections,
x_2: Normalized steering reversal rate of micro corrections,
and an additional new derived feature -
x_3: normalized steering reversal rate of macro corrections - normalized steering reversal rate of micro corrections.

Since the first two variables were found to be highly correlated with the third variable, as shown in the correlation matrix (fig :3.1), they were excluded from the feature set. Consequently, only the third variable was retained for Model 2 to reduce multicollinearity and improve model interpretability.

Model 3 -
x_1: Normalized steering reversal rate of macro corrections,
x_2: Normalized steering reversal rate of micro corrections,
x_3: normalized steering reversal rate of macro corrections - normalized steering reversal rate of micro corrections,
two additional new derived features -
x_4: rate of change of steering reversal rate of micro corrections

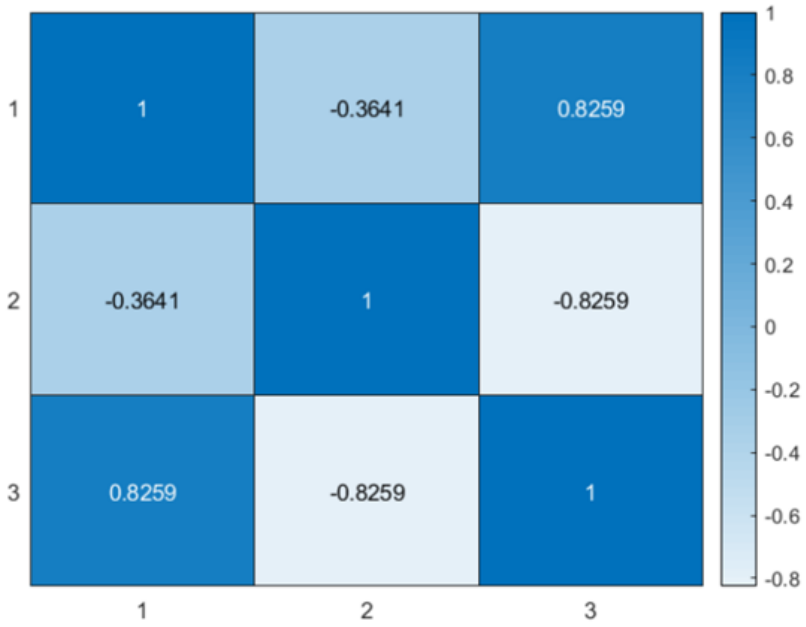

Figure 3.1: Correlation matrix between the initial three chosen features for Model 2

x_5: rate of change of steering reversal rate of macro corrections

Since the first two variables were highly correlated with the third one, as observed in the case of Model 3, only the third, fourth, and fifth features were retained. This selection aimed to reduce redundancy and mitigate the effects of multicollinearity in the model. Refer fig 3.3

Regarding the output variable—the Karolinska Sleepiness Scale (KSS) rating—it was simplified by introducing a binary classification scheme. A KSS rating of 7 was used as the threshold for drowsiness. Ratings equal to or above 7 were considered indicative of drowsiness and labeled as 1, while ratings below 7 were considered non-drowsy and labeled as 0. This transformation was essential, as logistic regression is a classification algorithm that requires a categorical output variable. Representing the output as binary values (0 and 1) enabled the model to effectively distinguish between drowsy and non-drowsy states.

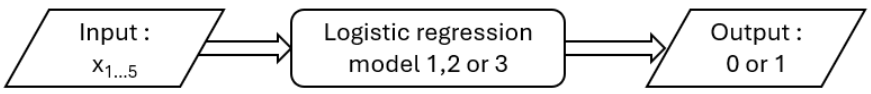

Figure 3.2: Block diagram representation of logistic regression model

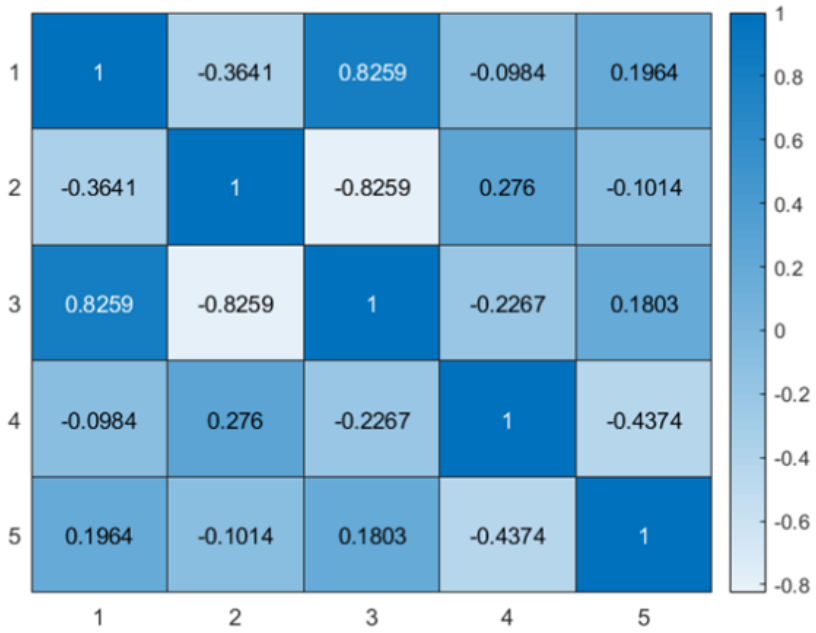

Figure 3.3: Correlation matrix between the initial three chosen features for Model 3

3.1.3 Model building and training

A logistic regression model is of the following form in general-

$$P(y = 1 \mid \mathbf{x}) = \frac{1}{1 + e^{-(\beta_0 + \beta_1 x_1 + \beta_2 x_2 + \cdots + \beta_n x_n)}}$$

where
$P(y = 1 \mid \mathbf{x})$: Probability that the output y is 1, given input vector $\mathbf{x}$,
β_0 : Intercept (bias term),
$\beta_1, \beta_2, \ldots, \beta_n$: Coefficients (weights) of the model,
$x_1, x_2, \ldots, x_n$: Input features,
e : Base of the natural logarithm

The three models were built in Matlab using the fitglm function. The basic syntax is as below -

```
mdl = fitglm(X, y)
```

where,

`mdl` : The fitted generalized linear model object. It contains model coefficients, diagnostics, and statistical summaries.

`X` : The matrix or table of predictor (independent) variables.

`y` : The response (dependent) variable.

All the models were trained using a 5-fold cross-validation technique. In this method, each dataset was randomly partitioned into five equal-sized subsets, or folds. Each model was trained on four folds and tested on the remaining one. This process was repeated five times for each model, with each fold used exactly once as the test set. The final model performance was then averaged over all five iterations, providing a more reliable estimate of accuracy or error rate. This approach helped reduce the risk of overfitting by evaluating the models on multiple data splits rather than a single train-test division. Additionally, it ensured that every data point was used for both training and testing, thereby improving the fairness and reliability of the performance assessment.
Since the output of the `fitglm` model is a probability score, a threshold was required to convert this continuous value into a binary classification of 0 or 1. Through trial and error, a threshold of 0.73 was selected, above which the driver was classified as drowsy.

The final models were -

Model 1>

$$\text{logit}(y) = 1.1 + 0.08x_1 - 0.14x_2$$

Model 2>

$$\text{logit}(y) = 1.1 + 0.12x_3$$

Model 3 >

$$\text{logit}(y) = 1.1 + 0.13x_3 + 0.05x_4 - 0.48x_5$$

logit(y) is a function that represents the logarithm of odds of an event. It is described as -

$$\text{logit}(y) = \log\left(\frac{p}{1-p}\right)$$

where

$$p = P(y = 1)$$

the probability of the event occurring.

x_1, x_2, x_3, x_4, and x_5 represent the predictor variables used in the individual models, as described in data preparation.

3.1.4 Model testing

The models were evaluated for their accuracy, sensitivity, and false positive rate.

Accuracy is the proportion of correctly classified instances (both positives and negatives) out of the total number of instances:

$$\text{Accuracy} = \frac{TP + TN}{TP + TN + FP + FN}$$

Sensitivity (also called recall or true positive rate) is the proportion of actual positive instances that were correctly classified:

$$\text{Sensitivity} = \frac{TP}{TP + FN}$$

False Positive Rate (FPR) is the proportion of actual negative instances that were incorrectly classified as positive:

$$\text{FPR} = \frac{FP}{FP + TN}$$

where,

TP is true positive
TN is true negative
FP is false positive and
FN is false negative

The metrics were further graphically represented using a receiver operating characteristic (ROC) curve. The ROC curve was used to evaluate the performance of the classification model by plotting sensitivity against the false positive rate at the classification threshold.

The results obtained from the three logistic regression models are analyzed and compared in Section 4: *Results & Discussion*. The discussion also highlights the impact of different feature selections on model effectiveness and offers insights into the strengths and limitations of each approach.

3.2 Real-time driver's steering behavioral understanding model

This model was developed by treating the test data as a time series. In this context, it was essential to account for changes in steering behavior rather than relying solely on absolute values. The logic behind developing this model was - if the reversal rates of micro-steering corrections decrease and simultaneously that of macro-steering corrections increase, then the driver is said to be drowsy, while the reversal rates of

micro-steering corrections increase and simultaneously that of macro-steering corrections decrease, then the driver is said to be less drowsy.

This model was developed in two phases: the learning phase and the detection phase.

3.2.1 Learning phase

The learning phase, as permitted by the regulation [3], was limited to a maximum duration of thirty minutes once the conditions for drowsiness detection were satisfied. In the learning phase, a probability density function was used to capture the overall distribution of how the driver changed the two parameters of micro and macro steering reversal rates within a specific recursive window size. A probability density function (PDF) describes the likelihood of a continuous random variable taking on a specific value. The PDF helps us understand how values are distributed over an interval, thereby aiding in the analysis of driver behavior.

The minimum threshold parameters for changes in the reversal rates of both micro- and macro-steering behaviors were learned from the probability density function (PDF) using the standard deviation method. For the reversal rate of micro-steering, a negative standard deviation from the mean value was considered, while for macro-steering, a positive standard deviation was used. This approach was based on the previously mentioned observation that a decrease in micro-steering correction rates combined with an increase in macro-steering correction rates indicates driver drowsiness. However, a maximum threshold was also determined from the PDF, as it was important to filter out rapid decreases or increases in the reversal rates of micro- and macro-steering corrections, respectively. Such abrupt changes may not necessarily be caused by drowsiness.
It can be noted that these thresholds are unique to each driver, based on their steering pattern.

3.2.2 Detection phase

During the detection phase, a trigger was generated if the changes in micro and macro steering reversal rates fell within the thresholds established during the learning phase, and the vehicle's speed exceeded 65 km/h for at least five minutes before and after the detection window. However, to issue a warning to the driver, more than two such triggers were required within the detection window—originating from both micro and macro steering reversal changes. This approach helped reduce the number of false positives. The warning to the driver was given with a delay of five minutes, once the above conditions were satisfied. No two warnings were issued within a period of five minutes.

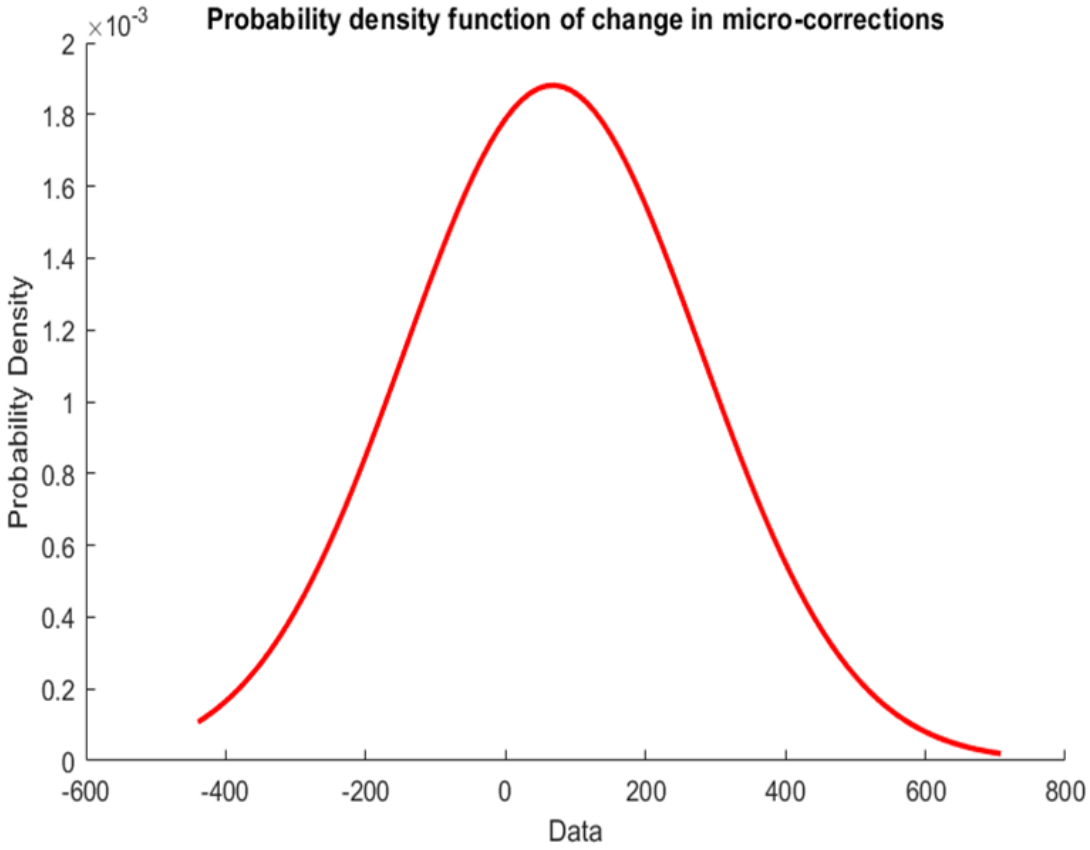

Figure 3.4: Example PDF of change in reversal rate of micro-corrections

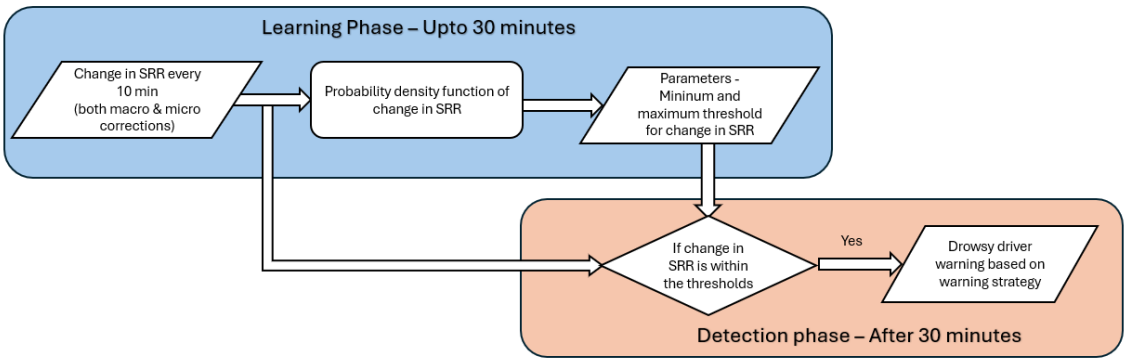

Figure 3.5: Block diagram representation of driver's steering behavioral understanding model

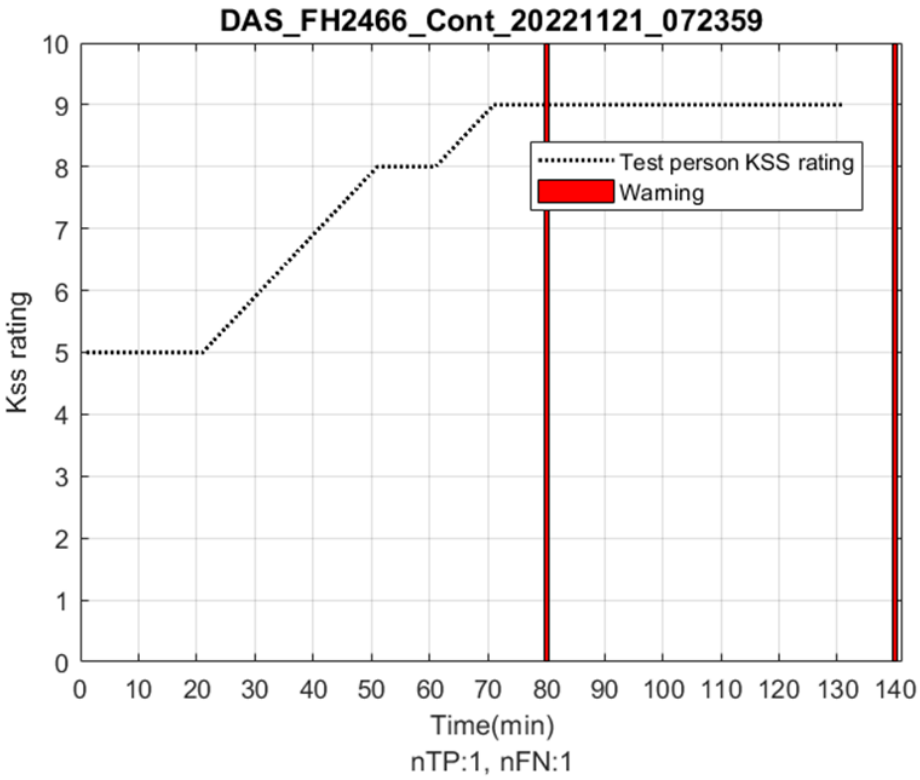

Figure 3.6: Atleast triggers within 5 minute window to give a warning

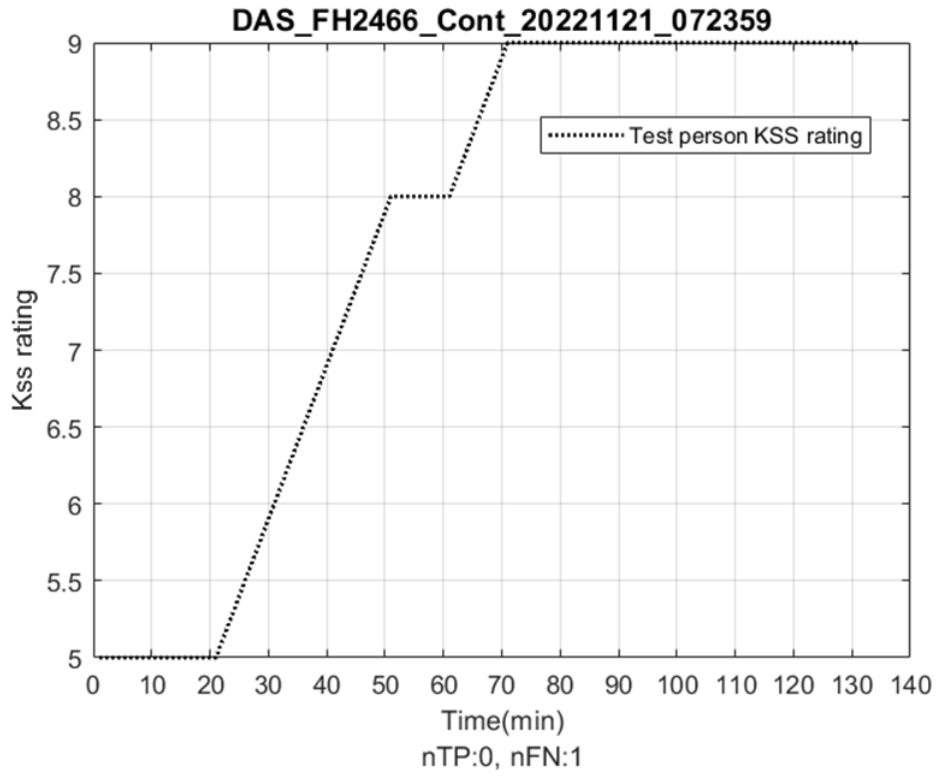

Figure 3.7: Atleast three triggers within 5 minute window to give a warning

It can be observed from figures 3.6 and 3.7 that if the warning strategy is changed, even by one trigger point, the final drowsy driver detection becomes more stringent. This can help in reducing the number of false positives (can be seen in Section 4: *Results & Discussion*)

4

Results & discussion

The results from the three algorithms discussed in the previous section are elaborated in this section.

4.1 Logistic regression model

Three logistic regression models that were built using different features had the following performance metrics (accuracy, sensitivity and false positive rate).

- Model 1

$$\text{logit}(y) = 1.1 + 0.08x_1 - 0.14x_2$$

where,
x_1: Normalized steering reversal rate of macro corrections,
x_2: Normalized steering reversal rate of micro corrections

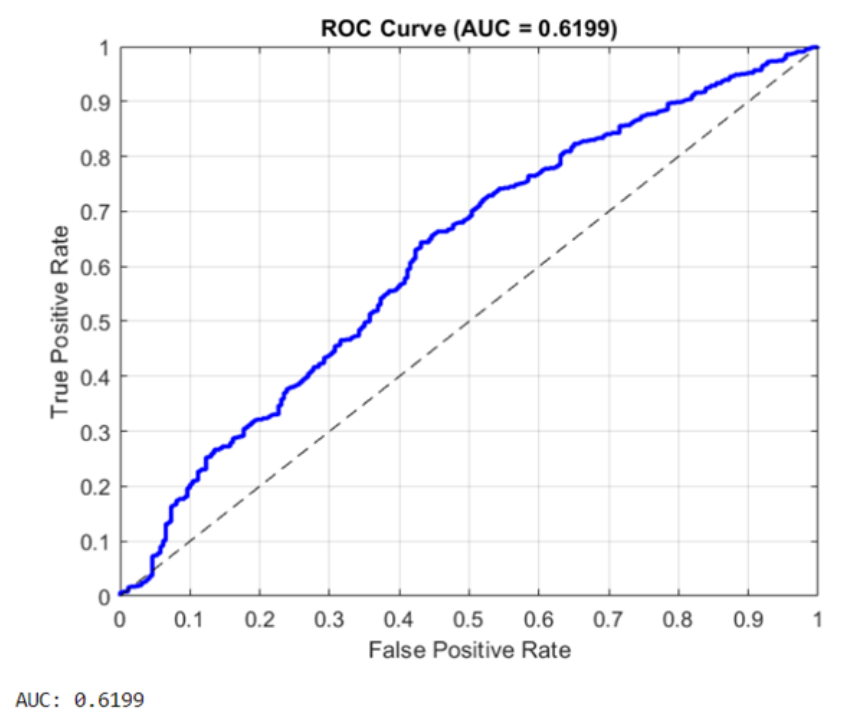

Figure 4.1: Area under curve of model 1

```
Generalized linear regression model:
    logit(y) ~ 1 + x1 + x2
    Distribution = Binomial

Estimated Coefficients:
                   Estimate       SE        tStat       pValue
                   ________    ________    _______    __________

    (Intercept)      1.0943    0.034655     31.577    7.6828e-219
    x1              0.079985    0.042882     1.8652      0.062148
    x2              -0.14058    0.033922    -4.1444    3.4078e-05
```

Figure 4.2: p-value of predictor variables of model 1

Accuracy = 0.71
Sensitivity = 0.82
False positive rate = 0.65

- Model 2

$$\text{logit}(y) = 1.1 + 0.12x_3$$

where,
x_3: normalized steering reversal rate of macro corrections - normalized steering reversal rate of micro corrections.

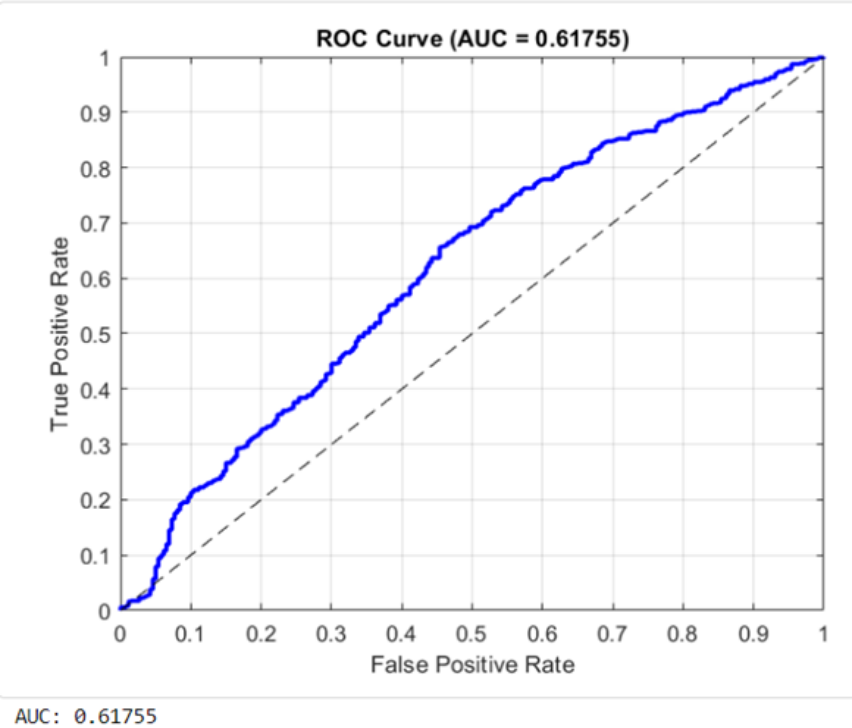

Figure 4.3: Area under curve of model 2

```
Generalized linear regression model:
    logit(y) ~ 1 + x1
    Distribution = Binomial

Estimated Coefficients:
                   Estimate       SE       tStat       pValue
                   ________    ________    ______    __________

    (Intercept)     1.0975      0.03474    31.593    4.5995e-219
    x1             0.12487     0.022116    5.6459     1.6428e-08
```

Figure 4.4: p-value of predictor variables of model 2 (here x1 is x_3)

Accuracy = 0.69
Sensitivity = 0.78
False positive rate = 0.60

- Model 3

$$\text{logit}(y) = 1.1 + 0.13x_3 + 0.05x_4 - 0.48x_5$$

where,
x_3: normalized steering reversal rate of macro corrections - normalized steering reversal rate of micro corrections,
two additional new derived features -
x_4: rate of change of steering reversal rate of micro corrections
x_5: rate of change of steering reversal rate of macro corrections

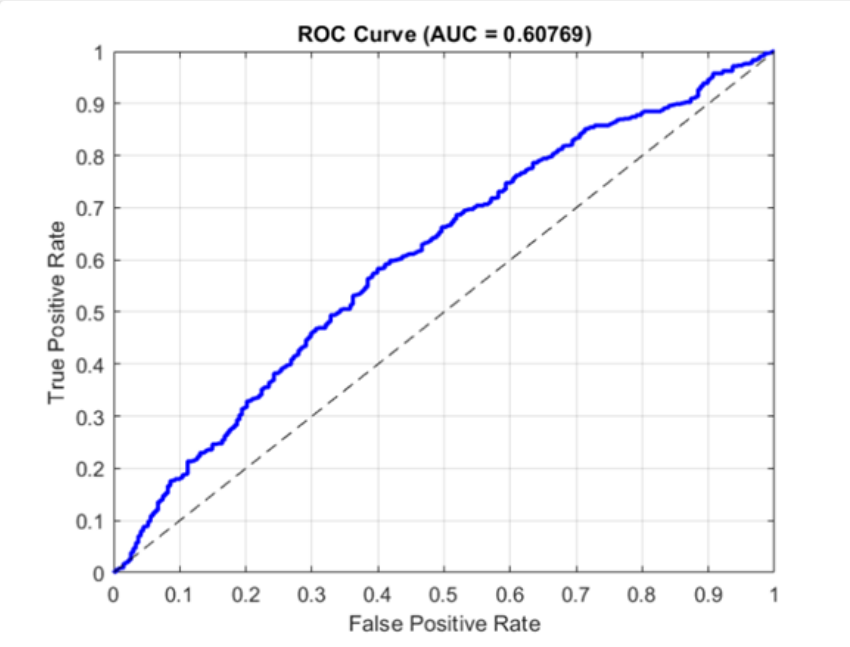


```
AUC: 0.60769
```

Figure 4.5: Area under curve of model 3

```
Generalized linear regression model:
    logit(y) ~ 1 + x1 + x2 + x3
    Distribution = Binomial

Estimated Coefficients:
                   Estimate       SE        tStat       pValue
                   ________    ________    _______    __________

    (Intercept)      1.1064     0.034825     31.77    1.6785e-221
    x1              0.12796     0.023573    5.4281    5.6972e-08
    x2             0.052755      0.12195    0.4326        0.6653
    x3             -0.48081      0.43536   -1.1044       0.26942
```

Figure 4.6: p-value of predictor variables of model 3 (here x1, x2 and x3 is x_3, x_4 and x_5 respectively)

Accuracy = 0.69
Sensitivity = 0.80
False positive rate = 0.67

It can be observed that the p-values associated with the predictor variables x_1, x_2, and x_2 are relatively small. This indicates that these variables are statistically significant in explaining the variation in the output variable. In contrast, the p-values for x_4 and x_5 are comparatively higher, suggesting that these predictors do not contribute significantly to the model. This finding is further supported by the box plots illustrating the relationship between x_4, x_5, and the output variable, where minimal variation in the output is observed with respect to median values of x_4 and x_5. These plots are presented below.

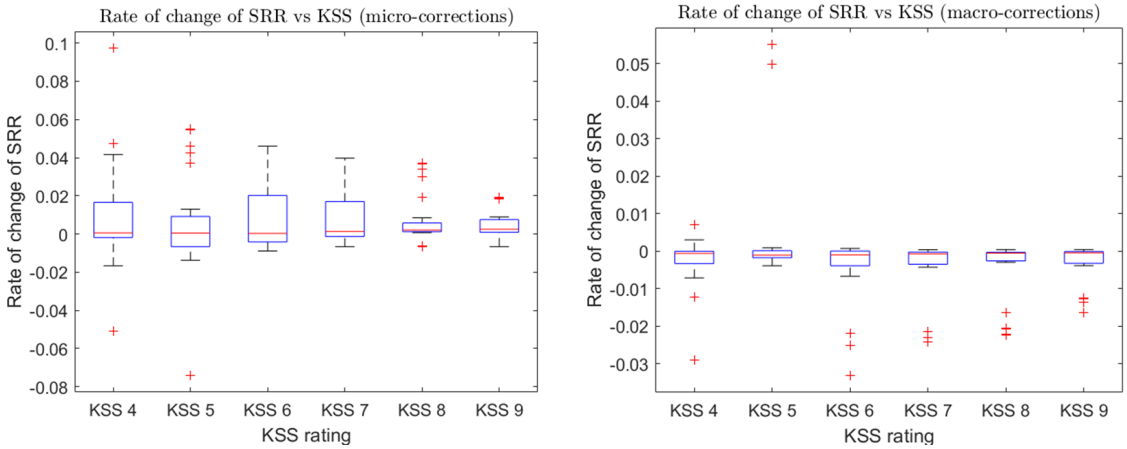

Figure 4.7: Predictor variable x_4 and x_5 vs output variable

Although the overall accuracy and sensitivity of all the models is relatively similar, the false positive rate serves as a key differentiating metric. Model 2 demonstrates the lowest false positive rate and, given that it relies on only a single predictor variable, it can also be considered the most parsimonious model.

However, a key limitation of the logistic regression approach is that a high false positive rate remains unacceptable, even when the model demonstrates high sensitivity.

This suggests that using the absolute values of micro- and macro-steering reversal rates to predict the Karolinska Sleepiness Scale (KSS) rating may not be a reliable method. These parameters are likely to vary significantly across individuals due to differences in driving styles, making it difficult to generalize the model effectively across all drivers.

4.2 Real-time driver's steering behavioral understanding model

The real-time driver's steering behavior understanding model was tested on two types of datasets: (1) drowsy driver test data and (2) non-drowsy driver test data.

The change in reversal rate of micro- and macro-steering was observed over a recursive window size of twenty minutes with a total learning time of thirty minutes. Although the function was designed to learn the driver behavior only when the vehicle speed is above 65 km/h, owing to the scarcity of total test data available, the function learned the driver behavior irrespective of time.

The following parameters were used in both test cases -

- Reversal rate of macro-corrections were defined at a gap size greater than 6°.
- Reversal rate of micro-corrections were defined at a gap size greater than 3°.
- Minimum threshold was defined at +1 standard deviation from the mean for macro-corrections and -1 standard deviation from the mean for micro-corrections.
- Maximum threshold was defined at +2 standard deviation from the mean for macro-corrections and -2 standard deviation from the mean for micro-correction.

The function was tuned in two ways -

1. At least three triggers from changes in both macro and micro corrections within the five minute window to give out a warning.
2. At least two triggers from changes in both macro and micro corrections within the five minute window to give out a warning.

Test case type	**At least two triggers for a warning**	**At least three triggers for a warning**
Drowsy data	75.69% sensitivity	64.73% sensitivity
Non-drowsy data	5/27 false positives	2/27 false positives

Table 4.1: Performance metrics of real time driver's steering behavioral understanding model

It is evident from the results that the sensitivity of the function remains high despite a very low number of false positives. Requiring more than two triggers from

both micro and macro steering corrections within a five-minute window to issue a warning makes the system more robust, reducing the number of false positives by 50% compared to the condition where at least two triggers are sufficient to issue a warning.

Since this method also takes vehicle speed into account for detecting driver drowsiness, it can be considered more reliable with fewer false positives. As illustrated in the diagrams below, it is noteworthy that only drowsiness causes an increase in the reversal rate of macro corrections and a decrease in the reversal rate of micro corrections when the vehicle speed exceeds around 65 km/h.

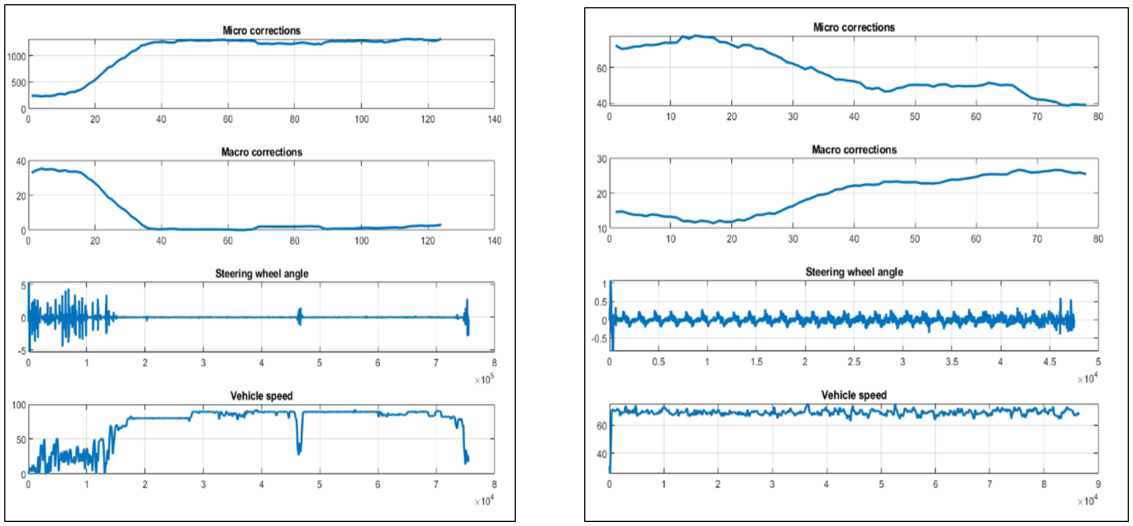

Figure 4.8: Trends in the vehicle metrics with time for non-drowsy and drowsy(right) drivers (ignore the scales)

5
Conclusion

The analysis demonstrated that driver drowsiness significantly affects steering behavior. Performance metrics—such as the average steering reversal rate for both micro and macro corrections, as well as the maximum values of key indices including steering wheel angle, steering wheel angle rate, yaw rate, and lane position—varied notably between low and high levels of drowsiness. Among the two secondary metrics, steering reversal rate proved to be a more reliable indicator of drowsiness than the key index, as the latter required extensive parameter tuning, which often altered the observed trends.

The distribution of these performance metrics varied across drivers, with some trends becoming more narrowly defined at higher levels of drowsiness. This indicates that while changes in steering behavior due to drowsiness were consistent across all drivers, the magnitude of those changes was unique to each individual.

To enhance the robustness of the analysis, vehicle speed was also incorporated as a critical variable. It was observed that, under non-drowsy conditions, drivers made more pronounced macro corrections and fewer micro corrections at lower speeds. Since the drowsy driving tests were conducted at speeds above 65 km/h, the observed increases in both macro and micro steering reversal rates could be attributed solely to increasing drowsiness. Therefore, including speed as a factor was essential for a more comprehensive and accurate assessment of driver behavior.

Between the two implemented methods—the logistic regression model and the real-time analysis of driver steering behavior—the former produced a high number of false positives. This was primarily because it relied solely on the absolute values of the steering reversal rate for both micro and macro corrections, in relation to drowsiness ratings. The logistic regression model used a fixed reversal rate threshold, assuming it to be universally applicable to all drivers. However, this approach failed to account for the fact that each driver has a unique driving pattern, which cannot be generalized.

In contrast, the real-time analysis model was designed to learn from individual driver behavior and establish personalized thresholds. This method effectively highlighted the uniqueness of each driver's steering behavior, which tends to persist even when the driver is drowsy. As a result, it provided more accurate and tailored assessments, reinforcing the importance of personalization in drowsiness detection systems. However, the limitation of this method is the speed threshold above which

driver drowsiness is detected.

In conclusion, the thesis successfully addressed all the research objectives outlined at the beginning, leading to the development of a reliable method for detecting driver drowsiness based on steering behavior.

6
Future work

As part of future work, the developed algorithm will be implemented and tested in real trucks to evaluate its efficacy. Additionally, other driver models will be explored to further enhance the detection of driver drowsiness.

Bibliography

[1] Risk assessment of road traffic accidents related to sleepiness during driving: a systematic review, Shehzad Saleem, Department of Community Medicine, King Edward Medical University, Lahore, Punjab, Pakistan

[2] Effects of driver task-related fatigue on driving performance, Massimiliano Gastaldi, Riccardo Rossi, Gregorio Gecchele, Department of Civil, Environmental and Architectural Engineering, University of Padova, Via Marzolo, 9, 35131 Padova, Italy

[3] COMMISSION DELEGATED REGULATION (EU) 2021/1341 of 23 April 2021

[4] A Steering Wheel Reversal Rate Metric for Assessing Effects of Visual and Cognitive Secondary Task Load. Gustav Markkula and Johan Engström, Volvo Technology Corporation

[5] Sensitivity of Lane Position and Steering Angle Measurements to Driver Fatigue. Hui Zhang, Chaozhong Wu, Zhen Huang, Xinping Yan, and Tony Z. Qiu, Transportation Research Record 2585

[6] Altmüller, T. Driver Monitoring and Drowsiness Detection by Steering Signal Analysis. PhD dissertation. Universität der Bundeswehr München, Munich, Germany, 2007

[7] Effect of Circadian Rhythms and Driving Duration on Fatigue Level and Driving Performance of Professional Drivers, Hui Zhang, Xinping Yan, Chaozhong Wu, and Tony Z. Qiu, Transportation Research Record 2402.

[8] Subjective and objective sleepiness in the active individual, T Akerstedt 1, M Gillberg, 1990

[9] Driver Alert Support Development Final Report, ER-540236,Peter Kronberg, 2009

DEPARTMENT OF MECHANICS AND MARITIME SCIENCES
CHALMERS UNIVERSITY OF TECHNOLOGY
Gothenburg, Sweden 2025
www.chalmers.se

CHALMERS
UNIVERSITY OF TECHNOLOGY